



UNIVERSITY OF LEEDS

This is a repository copy of *Tether monitoring for entanglement detection, disentanglement and localisation of autonomous robots*.

White Rose Research Online URL for this paper:

<https://eprints.whiterose.ac.uk/90764/>

Version: Accepted Version

Article:

Rajan, VAKT, Nagendran, A, Dehghani-Sanij, A et al. (1 more author) (2016) Tether monitoring for entanglement detection, disentanglement and localisation of autonomous robots. *Robotica*, 34 (3). pp. 527-548. ISSN 0263-5747

<https://doi.org/10.1017/S0263574714001623>

Reuse

Items deposited in White Rose Research Online are protected by copyright, with all rights reserved unless indicated otherwise. They may be downloaded and/or printed for private study, or other acts as permitted by national copyright laws. The publisher or other rights holders may allow further reproduction and re-use of the full text version. This is indicated by the licence information on the White Rose Research Online record for the item.

Takedown

If you consider content in White Rose Research Online to be in breach of UK law, please notify us by emailing eprints@whiterose.ac.uk including the URL of the record and the reason for the withdrawal request.



eprints@whiterose.ac.uk
<https://eprints.whiterose.ac.uk/>

Tether Monitoring for Entanglement Detection, Disentanglement and Localisation of Autonomous Robots

Vishnu Arun Kumar Thumatty Rajan¹, Arjun Nagendran², Abbas Dehghani-Sani³ and Robert C. Richardson³

¹*European Commission (EUROSTAT) Luxembourg, (e-mail:trishnuarunkumar@yahoo.com).*

²*Institute for Simulation and Training, University of Central Florida, USA (e-mail:arjun@cs.ucf.edu).*

³*School of Mechanical Engineering, University of Leeds, UK. (e-mail:[a.dehghani, R.C.Richardson]@leeds.ac.uk)*

Abstract: Tethered mobile robots are ideal for electrically noisy environments and for time-consuming tasks that require robust data communication and uninterrupted power delivery. However, tethers may become entangled in cluttered environments, leading to immobilization and consequent mission failure. This work addresses real-time monitoring of tethers to detect tether entanglement, perform disentanglement through tether following and localise within line of sight. Experimental hardware is proposed to implement the tether monitoring techniques. Experiments are performed for single and dual mobile robots to search a target environment and entanglement detection is shown to be successful using quantitative metrics such as mean localization error.

Index Terms— Tether, autonomous mobile robot, localization, entanglement, catenary curve.

I. INTRODUCTION

A tether is a multi-core cable that supplies a robot with power and communication capability. Tethered mobile robots have limited operational range (due to finite cable length) and are vulnerable to tether entanglement in cluttered environments. However, tethers are preferred for applications that are time intensive or within electrically noisy environments due to robust data communication and uninterrupted power delivery (Krishna et al. 1997, Remley et al. 2007, Ferworn et al. 2007, Abad-Manterola 2012). The reality of deploying un-tethered mobile robots is that battery life is very limited (under 2 hours in the majority of cases) and communications are frequently lost. Furthermore, when multiple un-tethered robots are deployed simultaneously, issues such as interference with other systems, data security and international band differences will arise (Fukushima et al. 2000). Therefore, the use of tethers has advantages in applications such as Urban Search and Rescue (USAR), reconnaissance, landmine detection, bomb disposal, planetary

exploration, sewerage and under-water exploration (Fukushima et al. 2000, Abel 1994, P.J. McKerrow et al. 2007). Fukushima et al. (2000) demonstrated that tethers can be used for climbing steep slopes (cliff-climbing) and for extracting robots when stuck in debris. Forces were applied to the end of the tether to in-turn apply forces to the robot dislodging it or reducing the effect of gravity. A tether connected between a robot and human allows a robot to follow human motions (Sangik et al. 2007) – this rationale is employed in this work, with a master-slave robot model for localization. When the tether is pulled by a user, the robot moves with linear and angular velocities proportional to the length and direction in which the tether is pulled. However, a drawback of this design is the limited working range ($\pm 30^\circ$) of the tether's orientation. A similar technique proposed by Kwan-Hoon et al. 2006 uses the tension and direction of the tether to control the linear and angular velocity of the robot. In our work, the tether is pulled taut and its direction is used for localization (line-of-sight) or detecting entanglement. Fukushima et al. (2000) proposed a follow the-leader type trajectory tracking system capable of estimating the position of a robot relative to its base interface.

Tethers have been proposed in space applications to control the momentum of a space robot. Chen and Cartmell (2007) proposed an interesting concept of accelerating a tether containing payloads attached to each end. As the tether is capable of exchanging momentum between the payloads, it is used as an orbital transfer system. Berenji et al. (1995) performed a simulation of satellite deployment and retrieval based on a mass-less model and a finite element model of a tether. Mori et al. (2000) proposed a method to estimate the relative position and attitude (pose) of the satellite based on tether length and tension. Table I compares and contrasts these approaches.

A tether disentanglement technique is proposed by Perrin et al. (2004) based on tether actuation induced by high pressure water transients formed by rapidly arresting its flow through the tether. The tether is capable of moving its own weight to overcome a locked condition. A similar comparison of locomotion using passive and active tethers is discussed by Yang et. al. (2009) where the “Water Hammer” effect is used to create jerks in the tether, thereby reducing the friction around entangled corners. However, there are only a few situations where the use of high pressure water would be possible.

An alternative approach to the tether entanglement problem is to precisely plan the robot's motion to avoid entanglement. Hert and Lumelsky (1999) devised a technique for the operation of multiple tethered robots where the robots move in a lower plane and the tethers are anchored in an upper plane. This approach requires a map of the

environment, complete information on the position of robot and tethers, and an environment where tethers can be anchored above the robots. These limitations present severe challenges to practically deploying the system. Disentanglement techniques proposed in this paper use ‘tether-following’ to help in localization.

TABLE I
ANALYSIS OF EXISTING TETHER MONITORING TECHNIQUES

| Tether Management Technique | Parameters Controlled | Limitations |
|------------------------------------|--|--|
| Sangik et al. | Tether length and orientation | Limited working range of tether’s orientation |
| Kwan-Hoon et al. | Tether tension and orientation | None specified |
| Fukushima et al. | Tether length and orientation | None specified |
| Chen et al. | Tether tension, momentum of payload | Only the design specifications are tested |
| Berenji et al. | Tether length and tension, longitudinal and vibrational oscillations | Simulation only |
| Mori et al. | Tether length, tether tension, relative position and attitude of the satellite | Only ground experiment, motion of each satellite is limited to 2D |
| Our Research Work | Tether length (l), tether tension (F), tether orientation (θ) | While tether following and entanglement detection have no limitations, localization requires line of sight |

| Tether Management Technique | Advantages | Target Applications |
|--------------------------------------|---|--|
| Sangik et al. | Able to follow the trajectory generated by the tether | Human-following robots |
| Kwan-Hoon et al. Fukushima et al. | Able to follow the trajectory generated by tether Tracking the position of a robot relative to a base interface | Human-following robots Follow-the-leader type trajectory tracking |
| Chen et al. | Propellant-less delivery of low mass | Insertion of a low-mass payload into the Earth’s atmosphere from a low-orbiting spacecraft |
| Berenji et al. | Mass-less model and finite element model of tether | Satellite deployment and retrieval for reuse |
| Mori et al. | Dynamic constellation of satellites | Various orbit service missions |
| Our Research Work | Tether following and entanglement detection do not require either an environment map or the robot to be localized. No environment map for relative localization and simple route map for global localization | Wide range of applications |

Iqbal et. al, (2008), present tether tracking and control of a robotic rover using a tether tension sensor and an IR sensor with an accuracy of 60mm. The need for tethers is justified as a source of both power and communications relay when operating the rover from a base station, however the authors do not consider entanglement obstacles or elaborate on details involved in their path planning algorithms. Since tethers form a physical connection between a reference point and a robot, it is theoretically possible to use the tether properties to find the robot’s position and orientation (i.e., localize it).

Localisation of mobile robots is important for successful navigation. Ideally, a detailed and accurate map would be known prior to deploying a robot and the robot would be able to reliably identify real features on the map and localise. However, there are many reasons why this is often not the case: (i) maps are not available quickly or do not exist, (ii) maps can contain errors (iii) damage to buildings or office renovations alter the building configuration (iv) robot sensors and intelligence is not sufficient to identify real features on the map.

Many of the techniques that have been proposed to solve the localisation problem are computationally intensive and often require expensive and large hardware such as laser scanners (Nagatani et al., 2003). Shang and Sun (2006) proposed a hybrid approach called MMK (Multi-sensory Markov-Kalman), which fuses a Markov model with a Kalman Filter (KF) using multi-sensory information. The MMK method benefits from the multi-modality of Markov for global localization and uni-modality of the KF for localization precision. This technique is aimed at structured office environments, where polyhedrons are used as features. Experiments are performed in a general indoor office environment.

TABLE II
EVALUATION OF EXISTING LOCALIZATION TECHNIQUES

| Research Work | Environment & Obstacle | Localization | Technique Used | Simulation or Real Robot |
|----------------|--------------------------|-------------------------------|----------------------------------|--------------------------|
| Nagatani et.al | Simple, static obstacles | Global (<i>Error-prone</i>) | Digital elevation map | Simulation |
| Nuchtet et.al | Medium, static obstacles | Global (<i>Too slow</i>) | Scan matching using loop closing | Real Robot |
| Howard at.al | Simple, static obstacles | Local (<i>Error-prone</i>) | Particle-filter | Real Robot |
| Shang at.al | Simple, static obstacles | Global | Multi-sensory Markov-Kalman | Real Robot |

The major limitations of this approach are that it uses sonar sensors that are noisy and error-prone, and the assumption of a simplistic environment. Table II summarises localisation techniques. None of these techniques use any prior knowledge. The aim of this work is to design, implement and analyse techniques and algorithms to reduce the problems associated with using tethers when deploying multiple mobile robots simultaneously. It is hypothesised that a mobile robot with the capability of unspooling its tether, pulling its tether cable taut (recoiling tether slack) and measuring the tether angle is capable of detecting tether entanglement through measurement of forces within the tether, localising within line of sight, and returning to an entry point by following the tether while it is recoiled. Figure 1 illustrates a tethered multiple robot search scenario with three robots. Without careful management of the tether motion, it is clear that the tethers are likely to become entangled around objects, other robots or restrict the robots' motion.

Crucially, the algorithms, techniques and hardware are designed to provide additional information with relative ease; many robots have the ability to unspool tethers (Wettergreen et.al, 1993, Hirose et.al, 2004, Mumm et.al, 2004) and with the addition of simple tether force sensors and/or tether angle measurements, vital performance data can be obtained. This work builds upon 2 pieces of preliminary work. The first developed the idea of using tethers to allow

robots to retrace their movements. This experiment was carried out using a single robot in a simple environment of two obstacles (Kumar and Richardson, 2008). The second developed the idea and presented preliminary results of using tether sag force to investigate entanglement of a tether between two robots (Kumar and Richardson, 2007). This work redefines earlier concepts to consider robots operating on uneven ground, provides detailed evidence of the quality of the results through detailed analysis and a case study of two robots. The contribution of this paper is in the experimental and analytical results of tethered mobile robots – no comparison to existing probabilistic approaches for localization such as the Monte Carlo localization technique (Thrun et.al. 2001) is made.

In section 2, applications of using tethered mobile robots and their management are presented. Section 3 details the theory of the work including equations for localisation and analysis of tether entanglement. In section 4 the design and trials experimental hardware for tether management are presented. Section 5 tests the hardware on mobile robots. Section 6 investigates disentanglement techniques. Section 7 presents case studies where these techniques have been implemented on single and dual robots. Finally, section 8 presents the conclusions of the work.

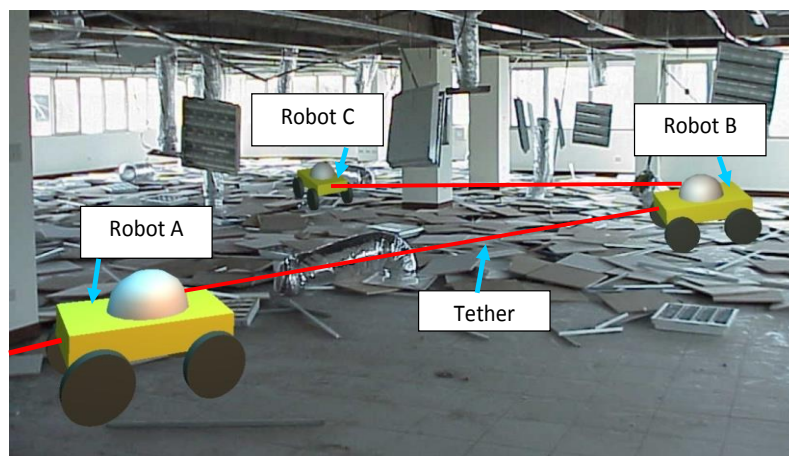


Figure 1: Tethered exploration with multiple robots

II. TETHER MANAGEMENT SCENARIOS

It is hypothesized that careful monitoring of tethers and their active manipulation will vastly improve the performance of tethered autonomous robots. Here, it is proposed that a tether recoil unit capable of winding cable and putting it under measurable tension, when combined with tether angle measurement can provide invaluable information for navigation.

The robots used here are based around small, cheap and simple designs that avoid the need for bulky expensive components such as 2D laser scanners required for SLAM (Simultaneous Localization and Mapping). In unstructured environments such as disaster zones that are characterized by debris fields and massive clutter, SLAM has limitations due to the nature of the returned data from laser scanners (point-cloud) and also requires complex hardware. Typically, robots in such environments are remotely operated and have little or no autonomy since there is no evidence of search and rescue robots having ever successfully performed full SLAM in such environments.

The deployment of sensors for tether management can be implemented in many ways. Here, several example scenarios are considered to examine the system properties:

Scenario A (disentanglement): A single robot contains an onboard spool of tether that can be unwound as the robot moves forward thereby avoiding dragging the tether. The robot contains an onboard tether angle measurement system. The robot can recoil the tether (wind it in) until it is taught and measure the tether angle so that the path taken can be retraced.

Scenario B: A single robot contains an onboard spool of tether that it uncoils as it moves forward. The robot can pull the tether taught and measure the tether angle. If the tether can be pulled to a straight line, localisation of the robot can be performed. A force sensor attached to the deployment point (start) measures the tether tension and algorithms determine if the tether is not obstructed.

Scenario C: A swarm of tethered robots may be deployed to explore a cluttered unknown environment (Figure 1). If several robots are connected together, power and communications can be transmitted via a grid system. Each robot contains a single onboard tether spooling unit and a single or multiple tether attachment points to other robots, with the tether tension measured by a force sensor. This allows localisation of the robot swarm. Indeed, multiple robots are more likely to have tethers within line of sight and therefore successful localisation is more likely.

There are many other applications where these techniques could be used including detecting an obstructed tether when a single robot moves through the environment dragging its tether (the robot contains onboard force sensor and start point an active tether spool), tethered underwater robots where line of sight is more probable, and localisation of tethered air vehicles such as blimps or quad-rotors.

III. THEORY

A. Entanglement detection

Entanglement is defined as a situation in which contact between the tether and external objects restricts the motion of the tether and hence impedes robot movement. It is proposed that by recoiling the tether until taut and measuring the transmitted force across the tether, restrictions on tether movement can be identified; a restricted tether will transmit forces to an external object and therefore a reduced force will be measured at the other end. Consider Figure 2 that illustrates two robots connected by a tether. Robot A contains a tether recoil unit and is capable of measuring tether sag angle. Robot B can measure the force at the tether attachment point and the tether sag angle.

Full entanglement (when the tether cannot be pulled taut across its whole length) is straightforward to detect due to low force transmitted across the tether. It is more difficult to detect partial entanglement that occurs when a tether is free to move, but rubbing against an object. In the partial entanglement the final transmitted force maybe close to that without entanglement. The following analysis is designed to detect both partial and full entanglement.

As the tether is recoiled, a graph can be produced of the tether length between robots and the associated tension across the tether. Comparison of the tether tension force and displacement curve to that of an ideal (not entangled) tether graph will reveal the entanglement state. Therefore, an ideal model of a tether is required. Previous researchers developed a lumped mass approach to model tether behaviour (Buckam and Nahon 1999). The tether is considered to be a system of point masses connected by visco-elastic springs. Here, the tether is assumed to be inelastic, allowing a simpler approach based around a catenary curve to be implemented.

The robots' tether attachment points are likely to be at different heights from the lowest point of the tether (O , referred to here as 'origin') (Figure 2). Therefore, the origin is not half way between the robots. It is assumed that the robots have on-board tilt sensors, therefore allowing compensation of any of the effects due to tilt on uneven terrain. The force and displacement graphs are obtained by recoiling the tether and measuring the force and tether length (L_c) at discrete intervals. The tether has to be freely hanging for the analysis to be valid.

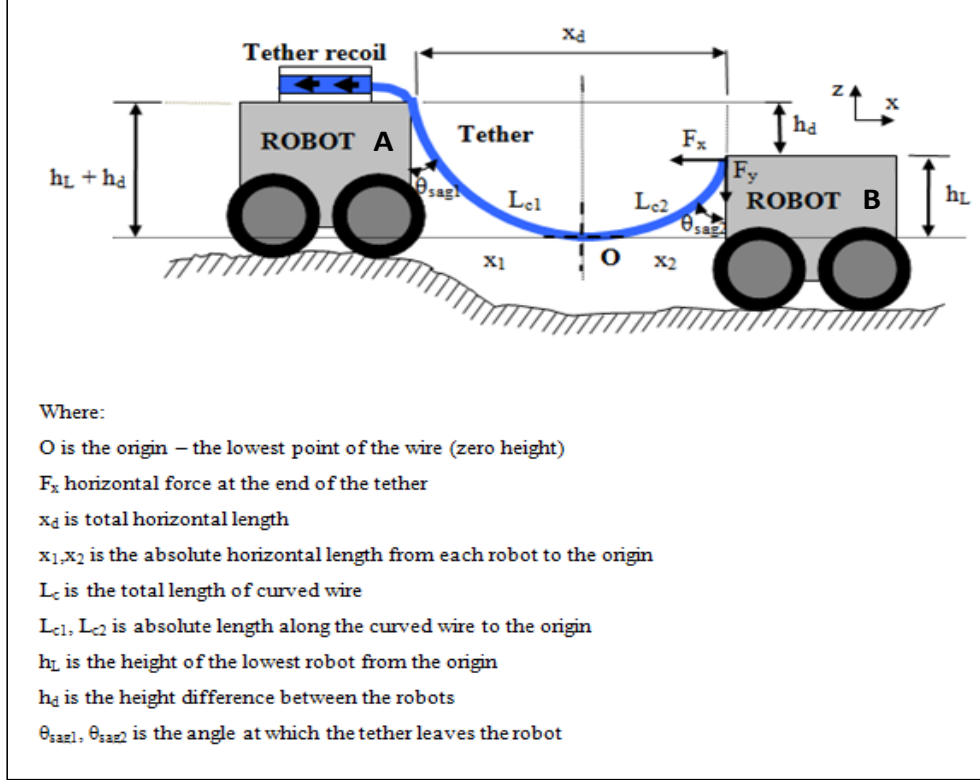


Figure 2: Tether tensioning arrangement

The analysis is split into two cases; 1) the robots are at the same height, and 2) the robots are at different heights. Case 1 is a specialized scenario that would only occur if the robots were operating on a flat surface, such as an office or warehouse. Case 2 is the more general scenario that is likely to be encountered.

Case 1: Robots at the same height

If the robots are at the same height, then ($h_d = 0$), $L_{c1}, L_{c2} = L_c/2 = L_s$; $x_1, x_2 = x_d/2 = x_s$ and $\theta_{sag1} = \theta_{sag2}$

$$L_s = a \sinh(x_s / a) \quad (1)$$

where ‘a’ is a parameter that scales the result determining the shape of the curve. The value of ‘a’ can be found by creating the following non-linear equation:

$$f(a) = L_s - \{a \sinh(x_s / a)\} = 0 \quad (2)$$

In order to use Newton-Raphson iterative method to solve the above equation, the derivative of f(a) is needed.

$$f'(a) = -\sinh(x_s / a) + \{(x_s / a) \cdot \cosh(x_s / a)\} \quad (3)$$

Assume the first guess $a_0 = L_h$, then

$$a_1 = a_0 - \left\{ \frac{f(a_0)}{f'(a_0)} \right\}, a_2 = a_1 - \left\{ \frac{f(a_1)}{f'(a_1)} \right\}, \dots$$

This is repeated until

$$\left(\frac{|a_{k+1} - a_k|}{|a_{k+1}|} \right) < \text{threshold} \quad (4)$$

The *threshold* can be as low as 10^{-5} . Lower the threshold, higher is the accuracy of the value of 'a'.

The horizontal pulling force F_{pull} is given by the following formula

$$F_{\text{pull}} = (q a) \quad (5)$$

where q = weight per unit length of the tether (N/m).

Case 2: Robots at different heights

In this scenario, the robots are at different heights. The aim of this analysis is to produce ideal graphs of force and displacement as the tether is recoiled, therefore no entanglement is considered in the analysis. The sag angles (θ_{sag1} & θ_{sag2}) can be obtained from onboard sensors. The variables h_d & x_d can again be obtained from a taut tether in the following equations.

$$L_c = L_{c1} + L_{c2} \quad (6)$$

$$x_d = x_{d1} + x_{d2} \quad (7)$$

As the tether is recoiled the tether length (L_c), sag angles θ_{sag1} , θ_{sag2} and horizontal force across the tether are measured. These measurements also reveal the robot with the greatest height. Van-Gessel (2011) defines equations to solve catenary curves at different supported heights (Equations (8) to (13)).

It can be shown that the horizontal distance is related to the tether length, height difference and height of the lowest robot as:

$$x_d = CD \quad (8)$$

where,

$$C = \frac{(L_c^2 - h_d^2)(h_d + 2h_L) \pm 2L_c \cdot \sqrt{h_L(h_d + h_L)(L_c^2 - h_d^2)}}{h_d^2} \quad (9)$$

$$D = a \tanh \left(\frac{h_d^2}{L_c(h_d + 2h_L) \pm 2\sqrt{h_L(h_d + h_L)(L_c^2 - h_d^2)}} \right) \quad (10)$$

Note that these equations are only valid when the robots are at different heights (i.e h_d cannot be equal to zero). During operation, if the equations become unsolvable, case 1 should be used. Equations (8) – (10) are used to obtain the height difference (h_d) for an experimentally measured horizontal distance between the robots (x_d) and measured tether length (L_c). The length of the tether from the robot to the origin can be found from the following equation:

$$L_{c1} = -\frac{h_L L_c \pm \sqrt{h_L(h_d + h_L)(L_c^2 - h_d^2)}}{h_d} \quad (11)$$

The horizontal force will be uniform across the tether (assuming the tether is flexible). The horizontal force can be shown to be:

$$F_x = \frac{\rho g (L_c^2 - h_L)}{2h_L} \quad (12)$$

Where ρ is the mass per unit length and g is the acceleration due to gravity. The vertical force is a result of the tether mass:

$$F_y = \rho g L_c \quad (13)$$

Note, that the forces F_x and F_y will need to be resolved depending on the inclination of the robot, as measured by its on-board sensors.

B. Localisation

An unrestricted tether under high tension will form a straight line between two robots. Under these conditions, the length of the tether and the start and end angles of the tether will define a kinematic path and allow relative localisation.

Figure 3 illustrates two tethered mobile robots deployed in an exploratory scenario. Each robot is equipped with a tether recoiling unit and is capable of placing the tether under tension. The tethers (under tension) and robot chassis form a path from the origin frame {0} to the end of Robot B (frame {9}). Frame {0} is treated as the ground station, from where the robots are deployed.

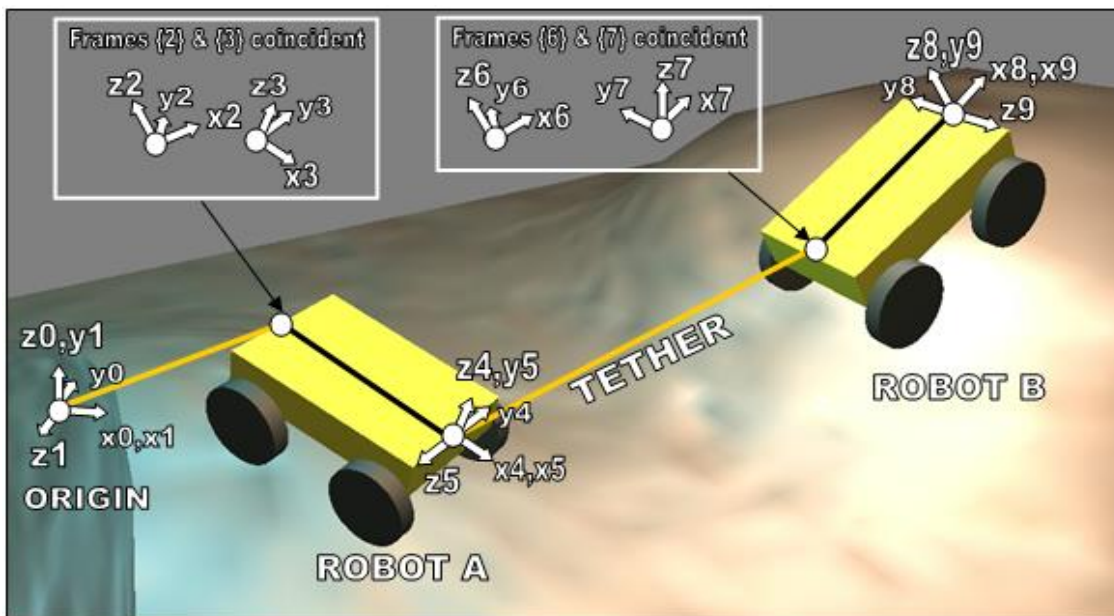


Figure 3: Localization of tethered mobile robots

A taut tether is susceptible to twist (roll along its length). The roll along the tether cannot be measured, therefore tether measurements alone are not sufficient to completely define the kinematic chain. A combination of sensors is proposed to overcome the inability to measure tether roll. Figure 4 illustrates the relationship between the sensors. At the start of a tether, a sensor is used to measure the yaw and pitch of the taut tether (figure 4a). At the end of the tether, a sensor is used to measure the relative yaw between the robot and tether (figure 4b). On-board the robot tilt sensors measure pitch and roll of the robot with respect to the global axis (figure 4c).

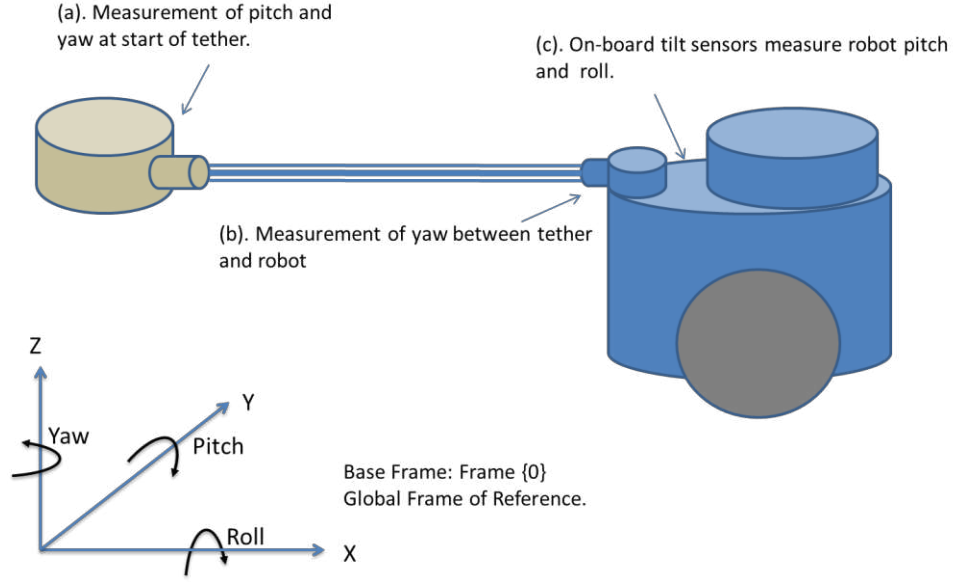


Figure 4: Kinematic analysis for tether-based localization

The following analysis demonstrates the validity of the proposed sensor scheme.

1. Frame {0} is the base frame. Frame {1} is aligned with the tether and is a pure rotation of frame {0}. φ_{y1} and φ_{p1} are the yaw and pitch required to align frame {0} with frame {1}. For simplicity of analysis, the undefined roll along the tether is modelled as a rotation between frames {2} and {3}. Therefore, frame {2} is a pure translation from frame {1} along the tether (L_1) (Figure 5). Note, frame {1} is not strictly required for the analysis, but is included for clarity. Equation (14) is the transformation between frame {0} and {2}, where the notation $c\varphi$ indicates $\cos(\varphi)$ and $s\varphi$ indicates $\sin(\varphi)$ in all equations that follow for brevity.

$${}^0T_2 = {}^0T_1 {}^1T_2 = \begin{bmatrix} c\varphi_{y1}c\varphi_{p1} & -s\varphi_{y1} & c\varphi_{y1}s\varphi_{p1} & L_1c\varphi_{y1}c\varphi_{p1} \\ s\varphi_{y1}c\varphi_{p1} & c\varphi_{y1} & s\varphi_{y1}s\varphi_{p1} & L_1s\varphi_{y1}c\varphi_{p1} \\ -s\varphi_{p1} & 0 & c\varphi_{p1} & -L_1s\varphi_{p1} \\ 0 & 0 & 0 & 1 \end{bmatrix} \quad (14)$$

2. Frame {3} is aligned with Robot A body and transitionally coincident with frame {2} (Figure 6) Frame {3} translation is therefore known in 3D space with respect to the global reference frame. However, at this stage, frame {3} pitch, roll and yaw are unknown (Equation (15), where X represents an unknown parameter).

$${}^0T_3 = \begin{bmatrix} X & X & X & L_1 c\varphi_{y1} c\varphi_{p1} \\ X & X & X & L_1 s\varphi_{y1} c\varphi_{p1} \\ X & X & X & -L_1 s\varphi_{p1} \\ 0 & 0 & 0 & 1 \end{bmatrix} \quad (15)$$

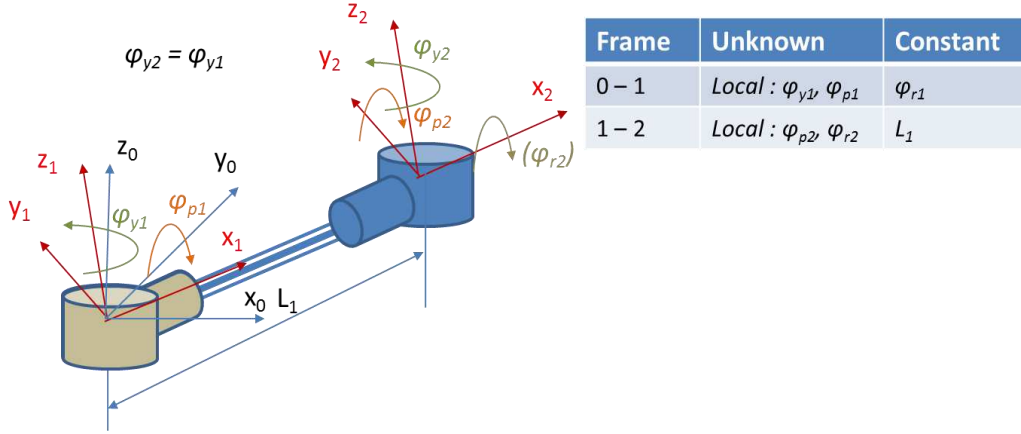


Figure 5: Transformation from frame {0} to {2}

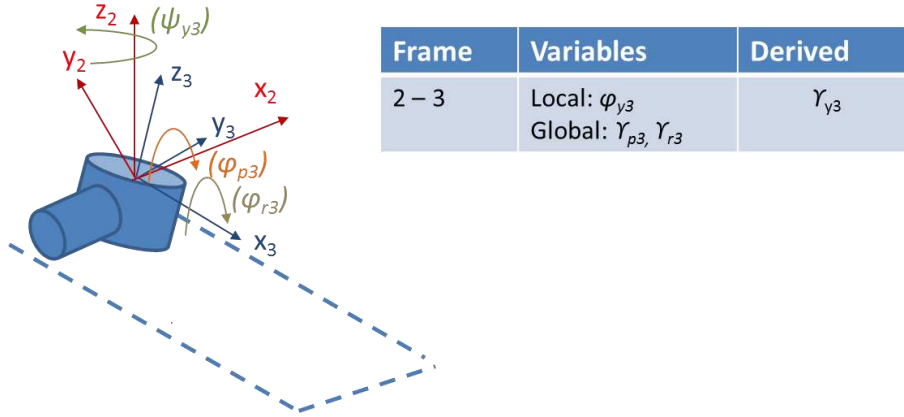


Figure 6: Translation from frame {2} to frame {3}

The global pitch and roll of robot A (γ_{p3} and γ_{r3} respectively) are obtained from onboard robot tilt sensors. The yaw between frames {2} and {3} (φ_{y3}) is measured locally with respect to the tether.

To find the global yaw of frame {3}, the locally measured yaw angle between frames {2} and {3} must be added onto the previous frame's global yaw rotation. Equation (16) extracts the global yaw of frame {2} from Equation (14) and Equation (17) then calculates the global yaw of frame {3}.

$$\gamma_{y2} = \text{atan2}(s\varphi_{y1}c\varphi_{p1}, c\varphi_{y1}c\varphi_{p1}) \quad (16)$$

$$\gamma_{y3} = \gamma_{y2} + \varphi_{y3} \quad (17)$$

The rotation matrix of frame {3} is then reconstructed from the global rotations (γ_{p3} , γ_{y3} and γ_{r3}). This rotation is then combined with the translation of Equation (15) to completely define frame {3} (Equation (18)).

$${}^0T_3 = \begin{bmatrix} c\gamma_{y3}c\gamma_{p3} & c\gamma_{y3}s\gamma_{p3}s\gamma_{r3} - s\gamma_{y3}c\gamma_{r3} & & \\ s\gamma_{y3}c\gamma_{p3} & s\gamma_{y3}s\gamma_{p3}s\gamma_{r3} + c\gamma_{y3}c\gamma_{r3} & \cdots & \\ -s\gamma_{p3} & c\gamma_{p3}s\gamma_{r3} & & \\ 0 & 0 & & \end{bmatrix} \quad (18)$$

$$\begin{bmatrix} c\gamma_{y3}s\gamma_{p3}c\gamma_{r3} + s\gamma_{y3}s\gamma_{r3} & L_1c\varphi_{y1}c\varphi_{p1} \\ \cdots & s\gamma_{y3}s\gamma_{p3}c\gamma_{r3} - c\gamma_{y3}s\gamma_{r3} & L_1s\varphi_{y1}c\varphi_{p1} \\ & c\gamma_{p3}c\gamma_{r3} & -L_1s\varphi_{p1} \\ & 0 & 1 \end{bmatrix}$$

The steps are summarized below:

1. **Rotate** about z-y-x (yaw, pitch, roll) to align frame {0} with frame {1}. i.e. 0T_1
2. **Translate** along frame {1} so that it coincides with frame {2} i.e. 1T_2
3. Find the rotation matrix of frame {3} through a combination of global orientation measurement and local yaw relative to the tether
4. Combine the rotation obtained in step 3 with the translation obtained in step 2 to fully define the location of frame 2.
5. Use standard forward kinematics to map from frame {3} to frame {4}

Repeat the process for additional robots.

C. Tether following and disentanglement

The tether forms a path from an entry point to the robot. If a robot recoils its tether while driving in the direction of the tether, it will retrace its steps and disentangle the tether from an obstacle (if the entanglement was as a result of robot motion and entanglement detection is performed regularly).

To perform tether following robots require obstacle avoidance and wall following algorithms alongside tether following techniques to prevent the robot following the tether into an object.

IV. EXPERIMENTAL EQUIPMENT

Experimental equipment was designed, constructed and tested to enable evaluation of the proposed tether monitoring techniques.

A. Robot hardware and sensing

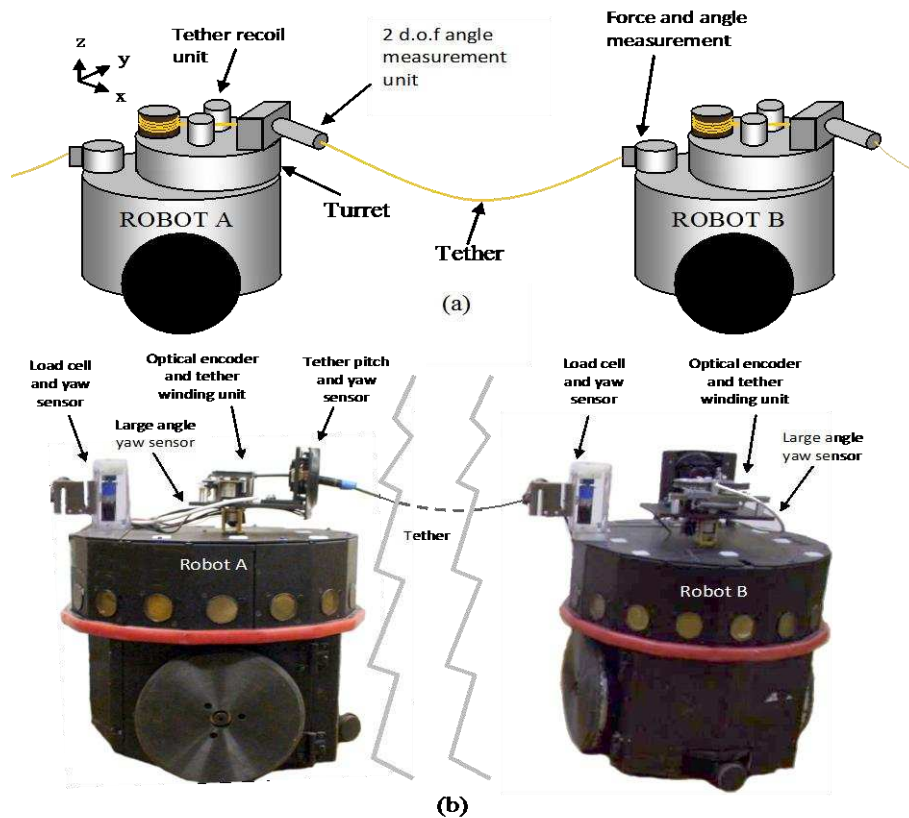


Figure 7: The proposed two robot system (a) illustration of concept (b) actual implementation

Two Nomad scout robots were modified for testing the tether management techniques. A Nomad scout has two differentially driven wheels, 16 ultrasonic sensors and 8 bumpers uniformly distributed. They are fully autonomous with an on-board computer, communication systems and batteries (not required in this application). Figure 7(a) shows a schematic of the tether monitoring hardware mounted upon two nomad scout robots and Figure 7(b) illustrates the actual experimental set-up.

Each robot has been augmented with a tether recoil unit to recoil slack tether and apply tension across the tether. Figure 8 illustrates the workings of the tether recoil unit. Two wheels are pulled into tension around the tether via a spring. One wheel is attached to a Maxon 6V, 5W motor, 370:1 gearbox ratio with a maximum output torque of 1.6Nm and the other is attached to an optical encoder. 1.6Nm and the other is attached to an optical encoder.

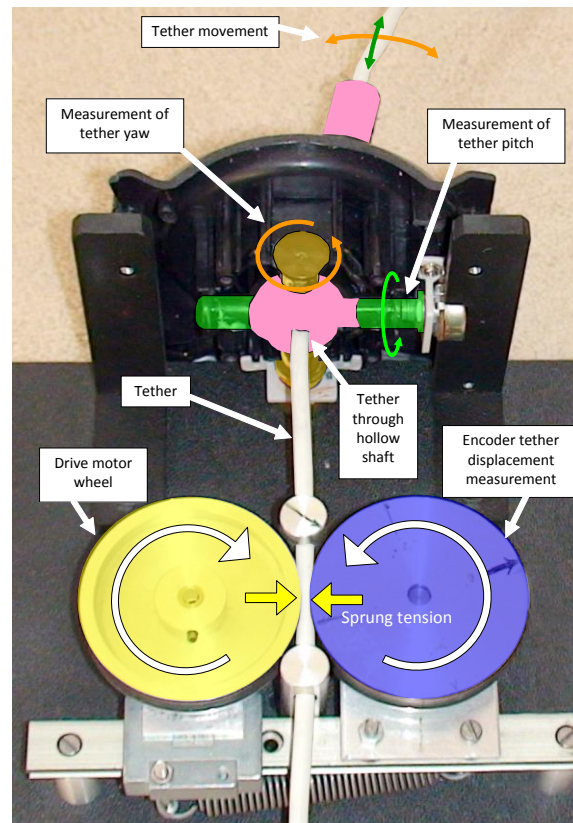


Figure 8: The tether winding system

When the motor is powered, the wheels turn pulling the cable. The length of the cable recoil is measured via the optical encoder. The driven and measurement wheels are not in direct contact, resulting in the encoder measuring the cable movement and not the motor rotation; therefore stalling of the cable recoil is easily detected and the recoil length is correctly measured. Small pitch and angles of the tether ($\pm 22.50^\circ$) are measured through a two degree of freedom measurement unit, with coincident points of rotation; this can be visualised as a two degree of freedom computer joystick with the tether passing through the handle (Figure 8). Large yaw rotation ($\pm 150^\circ$) is measured through a turret system between the tether winding unit and the robot. The combined small and large yaw angle measurement results in the actual angle. The measured tether pitch is the tether sag angle.

At the other end of the tether is a force sensor to measure the tension and a modular joint containing a yaw

measurement sensor and motor (the motor is an integral part of the modular joint, but is not powered in this work) (figure 9). The joint turns towards the tether when it is under tension due to the attachment offset. A tether of 15m length is used in these trials. A tether spooling system to store loose tether was not employed in these trials and would be required for actual deployment. The scout robots operate on a flat horizontal surface, therefore in this scenario, the equations for 3D localisation and entanglement detection at different heights reduce to a simpler form.

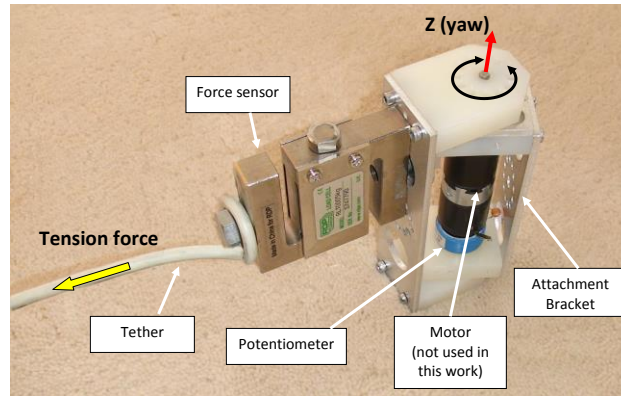


Figure 9: The tether tension and yaw sensor

One of the key aspirations of this work is that the technology should be affordable. Table III provides an indicative price for the component of the tether monitoring system. The overall price of £520 is the prototype cost and therefore could be reduced significantly if mass produced. The technology is relatively affordable when compared to the typical price of laser 2D rangefinders (£5K) or more sophisticated LADAR systems (£30K+).

TABLE III
INDICATIVE COMPONENT PRICES

| Unit | Components | Price (GBP) |
|--|-------------------|-------------|
| Tether winding unit and pitch/yaw sensor | DC motor | 50 |
| | Gearbox | 50 |
| | Wheel pair | 10 |
| | Platform | 10 |
| | Modified joystick | 30 |
| Tether tension and yaw measurement | Tension load cell | 150 |
| | Rotation joint | 20 |
| | Optical encoder | 90 |
| | Potentiometer | 10 |
| | Platform | 10 |
| Total | | 520 |

It must be noted that some of these technologies may however still be necessary depending on the context of robot operation (map building, obstacle detection etc.) and cannot be completely eliminated - in this case, one could combine

the tether management system described here-in with traditional localization techniques using sensor fusion to improve the accuracy of the localization.

B. Validation of experimental equipment and theory

Experimental trials were performed to measure the accuracy of the experimental hardware in measuring the tether length, localisation accuracy and tether force measurement.

Tether Length Measurement

The accuracy of the tether length measurement unit was evaluated through a test that wound and unwound a 15m long tether 10 times (300m of tether travel) and then comparing the measured length with actual length (measurements taken after 10 wind/unwind cycles). The experiment was repeated 20 times to determine the repeatability (6km of total travel). The measurement error during these trials was 1.65% with a standard deviation of 0.37%. It is possible to reduce this error by adding cable markings that can be optically measured and provide an absolute measurement of length and reset measurement drift.

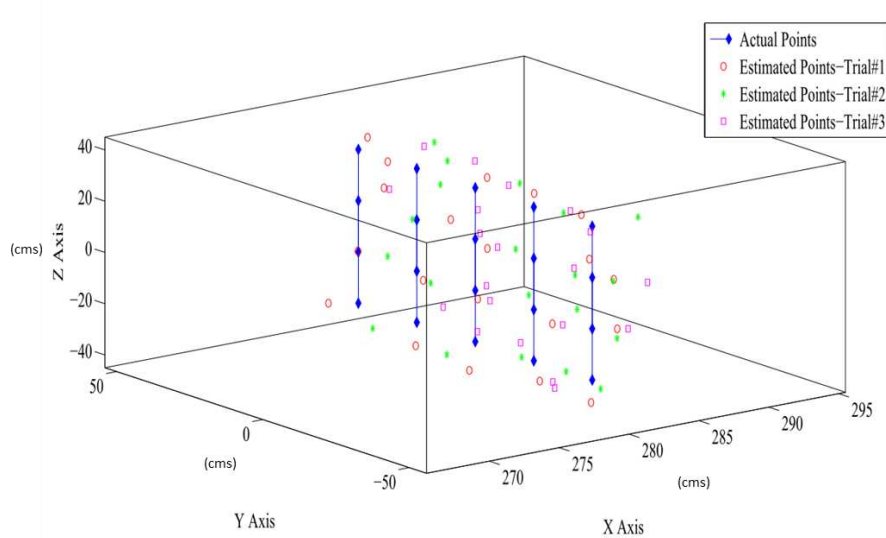


Figure 10: Actual and measured positions during 3D localization

Localisation accuracy

The tether angles and length were used to estimate the Cartesian coordinates of the tether end point. Twenty points were defined in 3D space.

The tether end was physically positioned at these coordinates and the actual coordinates compared with those measured by the tether measurement hardware. The actual and measured pitch and yaw values of the 3 trials were compared to find their average error percentages; these were found to be 2.5% and 1.7% with associated standard deviations of 0.46% and 0.37% respectively). Figure 10 illustrates the actual and measured tether end positions for three trials of twenty points using the tether length and angle (Kumar and Richardson 2007, 2008).

Force and length curves

An experiment was performed to validate the ideal (not entangled) theoretically predicted force as the tether is recoiled. Figure 11 (a) illustrates the measured force (F_x) and tether length (L_c) as a tether that is not entangled is recoiled ('No entanglement'). The experiment was performed at a distance of 10m horizontal distance (x_d). One way of interpreting the graph is to read it from right to left, to reveal the force across the tether as the tether lengths shortens (recoils). The graph shows excellent agreement between the measured force and ideal catenary curve forces. The graphs obtained during entanglement will be discussed in the next section.

V. ENTANGLEMENT DETECTION ON MOBILE ROBOTS

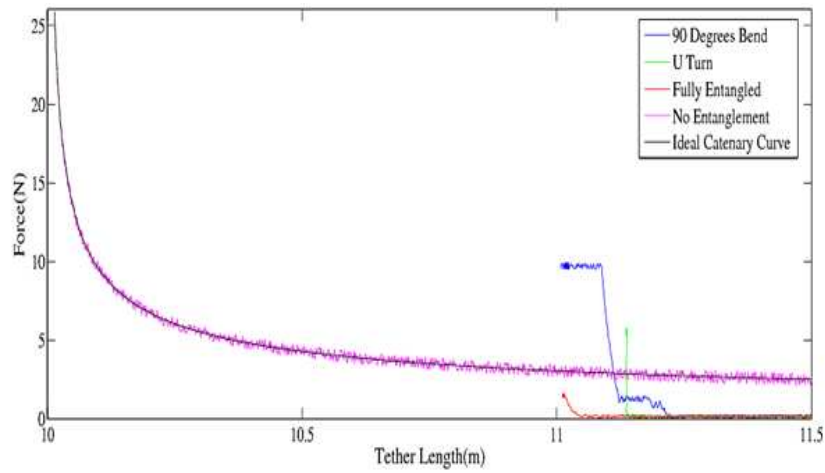
Two techniques for entanglement detection were evaluated. The first uses tether force data to predict entanglement and the second uses the tether global orientation to detect entanglement.

A. Force profiles for entanglement detection

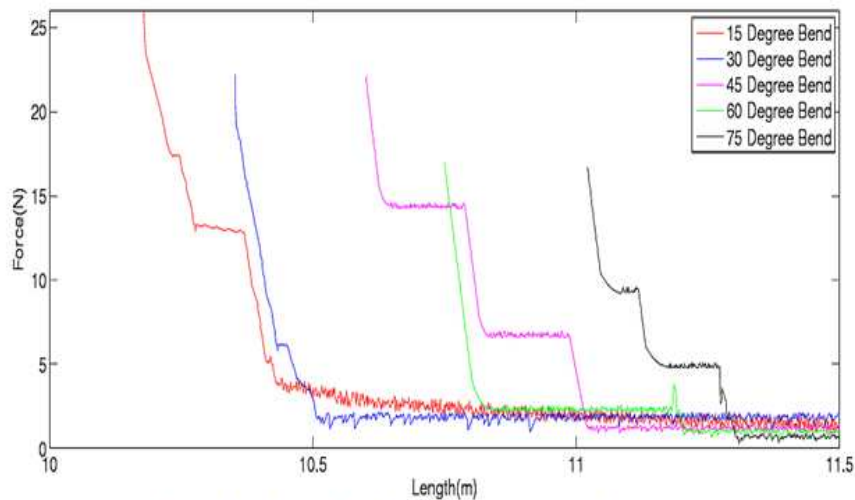
If there is no entanglement a significant proportion of the recoil force will be measured on Robot B. However, if the tether is restricted or entangled, less force will be transmitted and the transmission profile will be different. Therefore, based on the maximum force exerted on the tether and the pattern in which the force increases, entanglement can be detected. The standard deviation of force and length data from the ideal catenary curve can be used to measure how closely the force curve matches the theoretical curve.

Experiments were performed with robots on the same horizontal plane, with a 10m final length and three different initial tether lengths (11.5m, 12m and 12.5m). The tether was bent around an approximately circular piece of debris

at 9 different bend angles. Ten trials were performed for each initial length and obstacle; therefore 270 trials were performed in total.



a) Ideal curve, No Entanglement, Fully Entangled, U-Turn and 90 Degrees Bend Scenarios



(b) Tether bent through 15, 30, 45, 60 and 75 degrees from its straight line

Figure 11: Catenary force curves for a tether bent around a rough object for varying angles

Figure 11 (a) presents the length verses force curves for four scenarios of large bend angle variation along with the ideal catenary curve. The peak force is less than 2N for fully entangled case, as the winding force is predominantly applied to the obstacle. The peak force for U-Turn case (6N) (a bend angle of 180 degrees during entanglement) is less than that of the 90 degree bend case (10N), due to a greater normal force applied to the surface of the object, hence increased friction force.

The experimental curve for no entanglement case and the catenary curve closely follow each other. The initial force in this case is higher (~2N) compared to the entangled cases due to the weight of the freely hanging tether. The

measurement force oscillates more for a freely hanging tether due to tether oscillations. The plateau regions in the length and force graphs are as a result of stick-slip friction as the tether is dragged across the obstacle.

Figure 11 (b) represents the remaining five scenarios in which the tether is bent from its straight line through 15, 30, 45, 60 and 75 degrees around an obstacle. The higher the tether bend angle, the lower the peak force value due to increased normal friction force. Table IV shows that the force curve for the no entanglement case has the highest measured force value and the lowest standard deviation from the ideal catenary curve. There is a clear distinction between the no entangled and fully entangled scenarios and trend of decreasing measured force and increasing standard deviation for increasing bend angle. There is one exception to the trend where the standard deviation for a 360° bend angle (one full revolution) is lower than smaller bend angles. This is due to the constantly low transmitted value of force matching the initial low rise of the ideal catenary curve. Both the force and standard deviation would be good candidate variables to automatically detect entanglement; for example, if force is less than 25N then the tether has some entanglement. Determining the exact bend angle from measured force values (i.e a measured force value of 20N is approximately 35°) is inaccurate, therefore another approach is proposed to determine more precise measurements of tether angle.

TABLE IV
FORCE – RANGE AND STANDARD DEVIATION

| Bend angle (°) | Force (N) | | Standard Deviation (σ) | |
|---------------------|-----------|-------|---------------------------------|------|
| | MIN | MAX | Min | Max |
| 0 (No entangle) | 25.86 | 27.33 | 0.20 | 0.22 |
| 15 | 23.45 | 26.45 | 0.21 | 0.27 |
| 30 | 21.87 | 26.54 | 0.23 | 0.32 |
| 45 | 17.79 | 24.58 | 0.36 | 0.54 |
| 60 | 14.84 | 20.34 | 0.84 | 1.49 |
| 75 | 12.65 | 17.32 | 2.90 | 2.47 |
| 90 | 10.23 | 10.55 | 5.64 | 5.84 |
| 180 (U-turn) | 5.90 | 6.17 | 6.47 | 6.80 |
| 360 (full entangle) | 1.74 | 2.52 | 2.59 | 2.80 |

B. Entanglement detection through tether orientation

If the tether is recoiled to be under tension, the robot global orientation (as measured by a compass and inclinometers) along with the relative tether angles allow measurement of tether bend angle. If there is no entanglement, the tether forms a straight line and the tether angles, as measured on robots A and B will be aligned. Any misalignment of the tether angles is equivalent to the tether bend angle. An experiment of three trials with bend

angles ranging between 0 and 180 degrees was performed on the Nomad robots when operating on a flat surface. Table V presents the results of these tests.

The largest error of all of the trials was 1.40° . This principle can be extended to three dimensions if operating on uneven terrain. It should be noted that if tether cannot be pulled taut, this method may incorrectly measure no entanglement due to a loose tether randomly pointing in the correct direction; however this is unlikely.

TABLE V
TETHER ORIENTATION ANALYSIS

| Bend angle ($^{\circ}$) | Misalignment angle ($^{\circ}$) | | | Mean |
|---------------------------|-----------------------------------|---------|---------|-------|
| | TRIAL-1 | TRIAL-2 | Trial-3 | |
| 0 (no entangle) | -1.2 | 0.9 | 1.4 | 0.36 |
| 5 | 4.1 | 4.8 | 5.2 | 4.7 |
| 10 | 10.1 | 9 | 9.7 | 9.6 |
| 15 | 15.2 | 15.9 | 16.3 | 15.8 |
| 20 | 22.1 | 18.1 | 20.4 | 20.2 |
| 30 | 29.1 | 31.3 | 29.1 | 29.8 |
| 45 | 45.7 | 45.4 | 44.1 | 45.1 |
| 60 | 59.1 | 61.1 | 59.4 | 59.9 |
| 75 | 77.5 | 76.3 | 75.9 | 76.6 |
| 90 | 88.1 | 91.2 | 91.8 | 89.6 |
| 180 | 179.1 | 178 | 179.4 | 178.8 |

VI. DISENTANGLEMENT

To test the disentanglement strategy (scenario A) experiments were conducted consisting of a single robot following a tether through a cluttered environment. The objective of the disentanglement exercise is to establish the feasibility of the proposed approach in scenarios in which the entanglement is less than 360 degrees. To investigate this approach the nomad robots were programmed with a simple wall following algorithm; upon encountering an obstacle, the robot followed the wall of the obstacle (at a fixed distance using sonars) in the direction of the tether until the tether direction pointed away from the object.

Three experiments were performed in a 4.2m x 3m planar surface consisting of randomly placed objects with the tether intertwining between them (figure 12). The robot's traces (as directly measured at intermittent motion points) and the approximate initial tether states for the three scenarios are shown in figure 12. The traces indicate the centre of the robot. In scenarios-1, 2 and 3, specific instances with entanglement very close to 360 degrees have been introduced to make sure that the proposed disentanglement technique works under such worst-case scenarios. These instances have been marked as 'Critical Entanglement' in figures 12(a), 12(b) and 12(c). It is evident from figure 12 that the robot effectively achieves disentanglement by following the tether in all the instances in which the entanglement is less than 360 degrees.

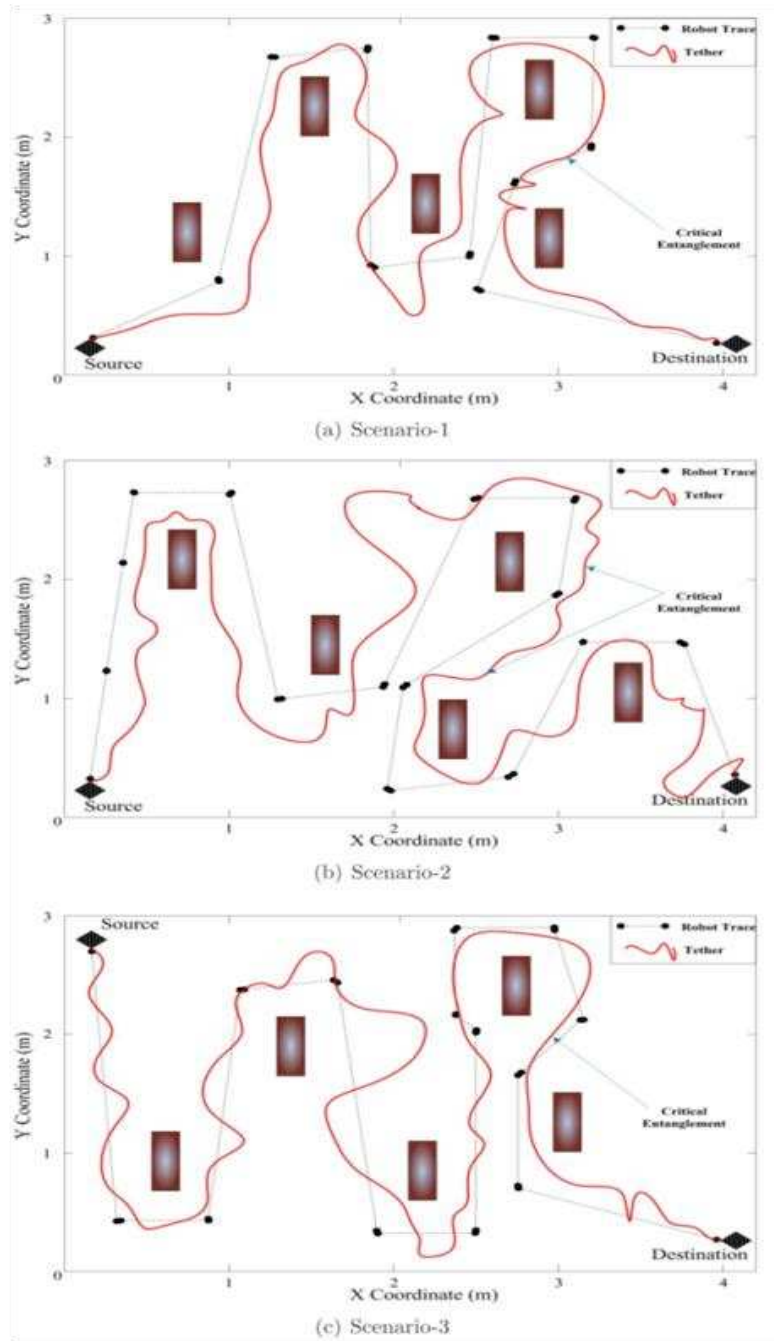


Figure 12: Disentanglement results for three obstacle scenarios

VII. CASE STUDIES

The techniques presented here have been implemented in two autonomous navigation case studies (single and dual robot) to further understand their performance and limitations. The robots were controlled by their own onboard computers.

The experiments were performed in a 4.2m x 3m planar surface consisting of obstacles and targets. The Nomad robots were programmed to perform a simple ‘zigzag’ target search using dead-reckoning (odometry-based). To perform a ‘zigzag’ search, the robot starts traversing the environment horizontally. When the robot reaches a horizontal search boundary it moves vertically a small amount and then traverses the environment horizontally in the opposite direction. This continues until the entire environment is explored. If obstacles are encountered during the motion (as detected by the ultrasonics), a simple avoidance strategy is implemented: The robot moves in a direction perpendicular to the obstacle (or the closest obstacle-free direction). Once the obstacle has been passed the robot resumes its search by travelling in a horizontal direction, as prior to performing obstacle avoidance. This may cause a portion of the search area to be left unexplored, depending on the obstacle size. It is assumed that a sensor will detect the target when the robot is 0.15m from the target. This is a very simple navigation strategy that is not suitable for a genuine search task. However, it is sufficient to analyse the performance of the tether management systems.

Setting up the thresholds for the entanglement detection parameters (force, standard deviation) depends on various factors like obstacle type, initial tether state and target applications. For these case studies, entanglement detection is triggered by force values lower than 20N and standard deviation values greater than 0.25N.

A. *Single Robot Case Study (Scenario B)*

A single robot case study was performed to assess the performance of the simplest possible system. In this scenario the robot is attached to an entry point and programmed to navigate through an environment comprising 2 obstacles and 2 targets. As the robot moves forward it unspools its tether. The robot frequently localises through pulling its tether taut. It is programmed to stop and localise once every 20 seconds, or when a target has been detected. The localisation attempts to implement entanglement detection based upon force measurement (section IV, case 1). The experiment was performed in three trials with two different obstacles placed at three different locations in the environment (18 experiments). A typical scenario for single robot case study is shown in Figure 13. If the robot detects an entanglement during the localization process, it disentangles itself by following the tether, while implementing a simple wall following algorithm to move around obstacles. Trials were performed using force based entanglement detection. The orientation method was applied post trial to the data assess whether failed attempts would be detected through this method.

Figure 14 shows the trace of the robot in a typical experimental trial. Note that this is the actual trace of the robot

motion plotted at specific time intervals by pausing the motion and precisely measuring the robot x, y position. The positions of the robot are numbered chronologically with respect to time.

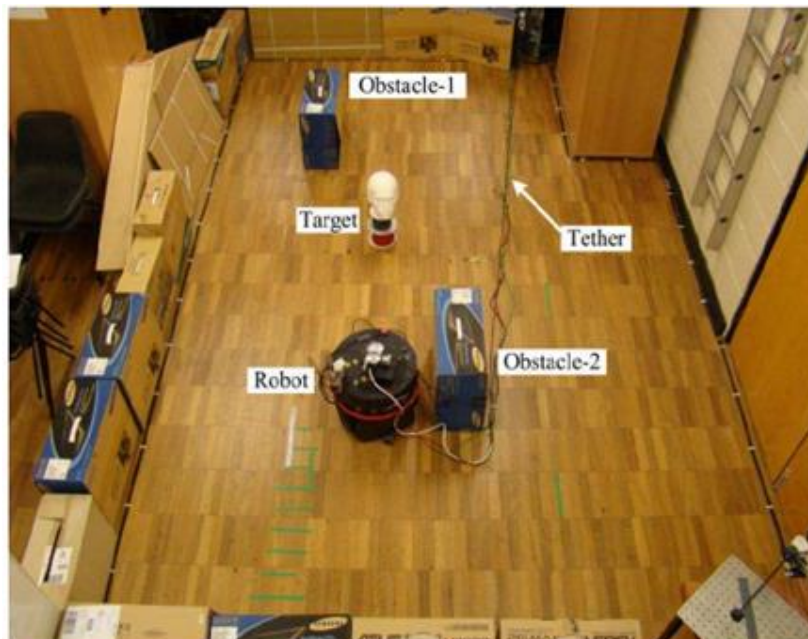


Figure 13: Single Robot Case Study - Experimental Scenario

The lines in Figure 14 are traces of the robot motion. The tether is not shown on the diagram for clarity, but its position (when not entangled) is a straight line from the robot to the entry point. The robot starts the zigzag search from the entry point at the bottom right corner, reaches position '1' and performs successful localization. After successful localisation in position '2', the robot follows and reaches the boundary of the search and moves to position '3'.

At position '3' tether entanglement is detected and the robot performs tether and wall following to reach position '4' where localisation is successful. A target is detected at position '5' causing the robot to perform localisation. The robot continues the journey to position '6' and then position '7'. At position '7', tether entanglement detection using force fails due to the small angle that the tether is bent through. Therefore the robot continues exploring until it detects entanglement in position '8'. It then performs tether and wall following to reach position '9' where localisation is successful. The robot then moves to position '10' and then detects a target at position '11' and localises. The robot completes the journey at position '12'. If orientation entanglement detection is applied in position '7' then entanglement is successfully detected and position '8' would be avoided.

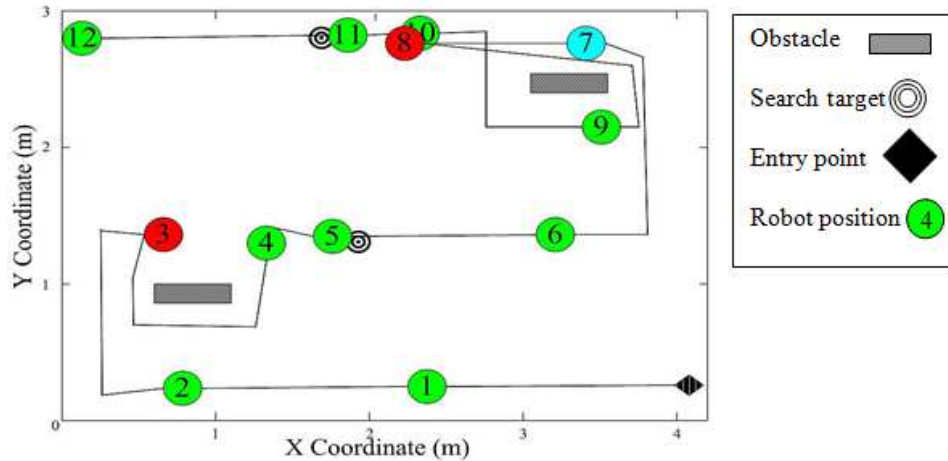


Figure 14: Schematic of the robot trial in an environment with obstacles

A. Dual Robot Case Study

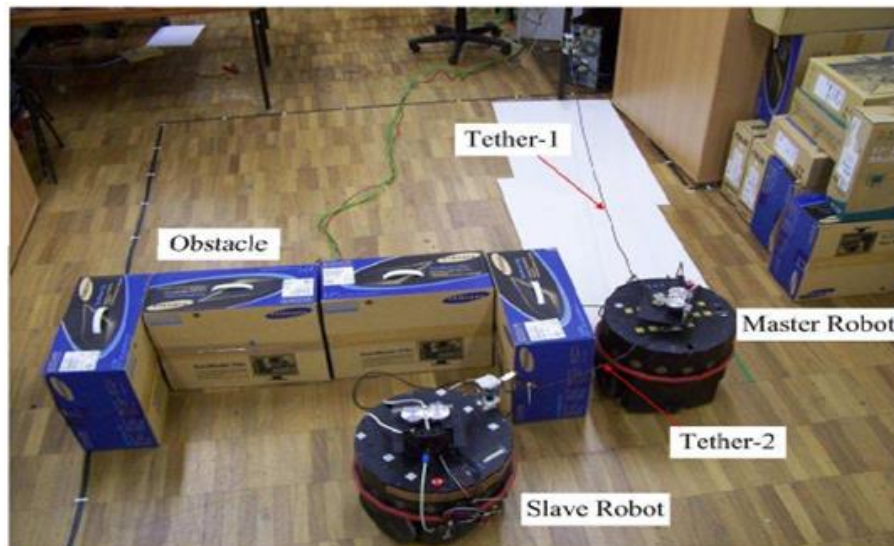


Figure 15: Dual Robot Case Study - Experimental Scenario

In this scenario two nomad robots are connected to an entry point via tether and tether management hardware. An inverted 'C' shaped obstacle was placed in the environment as an extreme challenge to the tether management system (Figure 15). For the dual robot search, an alternative search algorithm was implemented with the lead robot considered the slave and the following robot the master. The slave robot sweeps left and right at a set distance in front of the master robot. The master robot performs a 'zigzag' search as in single robot case study. The robots take it in turns to move, unspooling tether as they do, and then recoiling the tether intermittently to localise.

Both robots implement obstacle avoidance and tether/wall following when the situations of obstacle or tether entanglement occur.

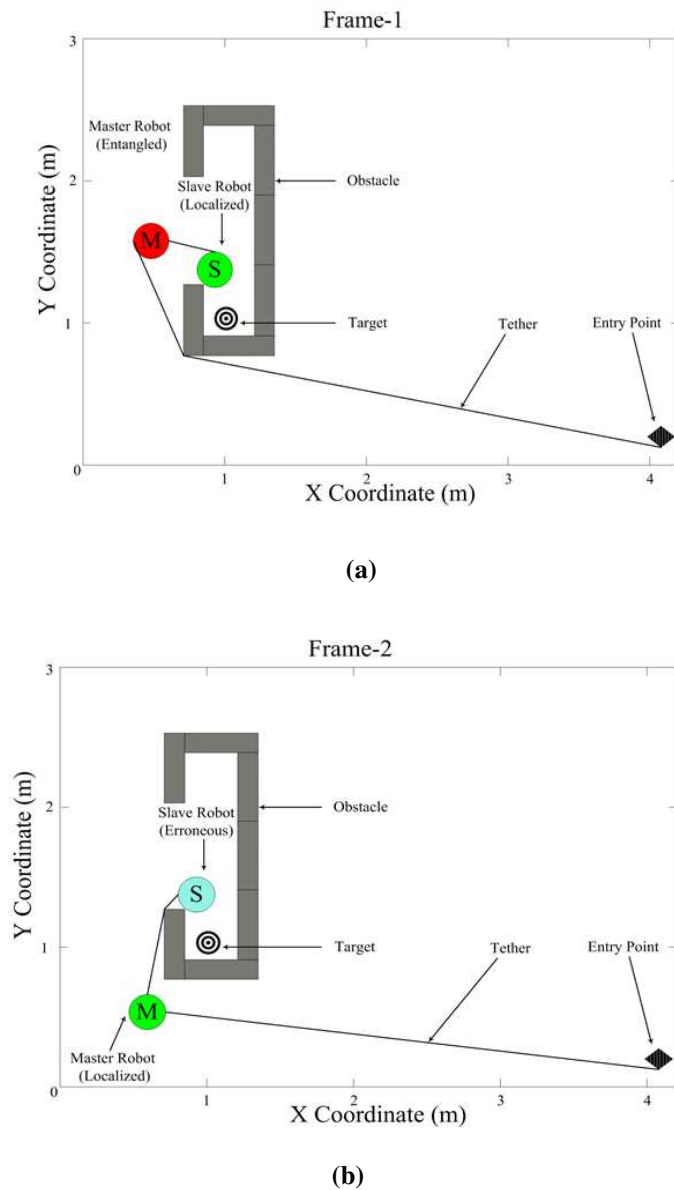


Figure 16: Handling complex obstacles. (a) Situation where slave robot is relatively localizable with respect to the master, but localization is not possible due to master robot entanglement. (b) Situation where master robot is localized, but slave robot localization is erroneous due to entanglement.

The environment has one complex obstacle and one target hidden within the obstacle. Figure 16(a) shows a typical experimental scenario where line of sight is maintained and Figure 16(b) depicts a trial in which the entanglement detection based on force fails. For the failure case (Figure 16(a)), the slave robot is relatively localisable with respect to the master robot, however the master robot tether is entangled and therefore localisation is not possible. To

disentangle itself, the master robot follows the tether, until it reaches the wall of the obstacle and then it moves diagonally backwards as shown in Figure 16(b). At this point entanglement detection based upon the force measurement fails for the slave robot, as the tether is only slightly bent by the obstacle. The system assumes that there is no entanglement and presents erroneous target position value. Tether orientation analysis detects the entanglement illustrated in (Figure 16 (b)). A series of experiments were performed to analyse the performance of dual robots further. Three trials with obstacles of four different shapes (T-shaped, V-shaped, Square-cap-shaped, enclosed square cap shaped) were placed at 2 different locations in the environment (24 samples). The outcomes of these trials and the single robot trails are presented in the analysis section (Section C).

B. Analysis of multiple trials

The mean localization errors for every localization event in both the single and dual robot case studies are 4.8cm (0.96%) and 6.8cm (1.36%) (Standard Deviation 0.22% and 0.29%) respectively, for a maximum range of 5m. Table VI presents the success rate of the entanglement detection and disentanglement techniques in the case studies. The number of events represents the total number of experimental samples available for a specific tether management technique. The column ‘Success’ shows how many times the technique was successfully performed and ‘Fail’ shows the failure count in entanglement detection or disentanglement techniques. The entanglement detection based upon force model and orientations were applied to every entanglement scenario. During the robot trials, not every entanglement resulted in a disentanglement attempt; therefore there are less disentanglement attempts compared with the entanglements detected.

The failures in force entanglement detection were all as a result of tether bends less than 60° . Therefore, the success rate depends on the size of the bend in the tether and also careful selection of entanglement force and standard deviation values. The success rates of the entanglement detection based on tether orientation analysis, robot recovery (tether following to an entrance point) and disentanglement by tether following are 100% each. On a larger sample of data, orientation analysis alone would occasionally fail due to full tether entanglement and a randomly correct tether direction.

TABLE VI
SUCCESS RATE (FORCE = 20N, STANDARD DEVIATION = 0.25N)

| Case study | Event | Overall no. of events | Success | Fail | Success Rate (%) |
|------------|-------|-----------------------|---------|------|------------------|
|------------|-------|-----------------------|---------|------|------------------|

| | | | | | |
|--------------------------------|--|-----|-----|----|-------|
| | Entanglement Detection (<i>force Model</i>) | 201 | 195 | 6 | 97.02 |
| | Entanglement Detection (<i>Tether Orientation</i>) | 201 | 201 | 0 | 100 |
| Single Robot Case Study | Disentanglement | 36 | 36 | 0 | 100 |
| | Robot recovery | 18 | 18 | 0 | 100 |
| | Entanglement Detection (<i>force Model</i>) | 749 | 731 | 17 | 97.73 |
| | Entanglement Detection (<i>Tether Orientation</i>) | 749 | 749 | 0 | 100 |
| Dual Robot Case Study | Disentanglement | 48 | 48 | 0 | 100 |
| | Robot Recovery | 48 | 48 | 0 | 100 |

The major limitation in the case studies is that the robot can localize only when it is in direct line of sight without any intervening obstacles. This limitation can be tackled by using multiple robots forming a tree-like structure exploring the environment. An approach of force and orientation analysis could produce a robust system: (i) if the force entanglement detection is performed initially to look for entanglement greater than 60° (ii) if no entanglement is detected on the force method the orientation approach is used to look of small angles of entanglement. Using this technique orientation analysis would only be performed when the tether is taut as measured by force entanglement detection.

VIII. CONCLUSION

A low-cost and robust tether management system has been proposed. The system does not require an environmental map for its operation and offers a wide range of advantages; such as localization and robot recovery. It also reduces the inherent problem of entanglement associated with a tether by detection and disentanglement. The work has demonstrated the feasibility of the approach both theoretically and in practical reality. The technique has limitations in that it requires additional hardware, the robots to be primarily in line of sight, and the catenary force curve approach has limited applicability for very short robots. Two case studies were presented to verify the validity of the proposed approaches. These case studies demonstrated multiple autonomous robots detecting and escaping from tether entanglement for the first time. The work has demonstrated that useful information can be relatively easily be obtained

from force and angle sensors attached to tethered mobile robots and therefore the measurement principles developed here should be considered for inclusion on all tethered robots. Future work will implement these techniques in 3D and on swarms of robots.

REFERENCES

- [1] Krishna M, Bares J, Mutschler E, Tethering system design for Dante-II. Proceedings of IEEE International Conf. on Robotics and Automation. Vol.2, Page(s) 1100–1105, Albuquerque, NM, 20-25 April 1997.
- [2] Remley K, Koepke G, Messina E, Jacoff A, Hough G. Standards development for wireless communications for urban search and rescue robots. International Symposium on Advanced Radio Technology. Boulder, Colorado, Page(s) 66-70, Feb 26-28 2007.
- [3] Ferworn A, Tran N, Tran J, Zarnett G, and Sharifi F, Wifi repeater deployment for improved communication in confined-space urban disaster search, in Proceedings of IEEE International Conference on System Engineering. Page(s) 1-5. San Antonio, TX, 16-18 April 2007.
- [4] Fukushima EF, Kitamura N, Hirose S. A new flexible component for field robotic system. Proceedings of IEEE International Conference on Robotics and Automation. Vol.3, Page(s) 2583-2588, 24-28 April 2000.
- [5] Sangik N, Hyo-Sung A, Yu-Cheol L, and Wonpil Y. Navi-guider: An intuitive guiding system for the mobile robot. Proceedings of IEEE International Symposium on Robot and Human interactive Communication (RO-MAN). Jeju, Page(s) 228-233, 26-29 August 2007.
- [6] Kwan-Hoon K, Jun-Uk C, Yun-Jung L. Steering-by-tether and modular architecture for human-following robot. Proc. of International Joint Conference SICE-ICASE. Page(s) 340-343, Busan, 18-21 Oct 2006.
- [7] Chen Y, Cartmell MP., Multi- objective optimisation on motorised momentum exchange tether for payload orbital transfer. Proceedings of IEEE Congress on Evolutionary Computation. Page(s) 987- 993, Singapore, 25-28 Sept. 2007.
- [8] Berenji HR, Malkani A, Copeland C. Tether control using fuzzy reinforcement learning. Proceedings of IEEE International Conference on Fuzzy Systems. Vol.3, Page(s) 1315-1322, Yokohama, Japan, 20-24 March 1995.

- [9] Mori O, Matunaga S, Waeda N. Research and development of tethered satellite cluster systems. Proceedings of IEEE/RSJ International Conference on Intelligent Robots and Systems. Vol.3, Page(s) 1834- 1840, Takamatsu, Japan, 31 Oct – 5 Nov 2000.
- [10] Perrin DP, Kwon A, Howe RD. A novel actuated tether design for rescue robots using hydraulic transients. Proceedings of the IEEE International Conference on Robotics and Automation, Cambridge, Page(s) 3482-3487, 26 April - 1 May, New Orleans, USA, 2004.
- [11] X. Yang, R. Voyles, K. Li, and S. Povilus, “Experimental comparison of robotics locomotion with passive tether and active tether,” in Proc. IEEE Int’l Workshop on Safety, Security and Rescue Robotics, 2009
- [12] Hert S, Lumelsky V. Motion planning in R3 for multiple tethered robots. IEEE Transactions on Robotics and Automation. Vol.15, Page(s) 623-639, Grenoble, France, 7-11 Sept. 1999.
- [13] J. Iqbal, S. Heikkila, and A. Halme. Tether tracking and control of ROSA robotic rover. In Control, Automation, Robotics and Vision, 2008. ICARCV 2008. 10th International Conference on, pages 689–693. IEEE, 2008
- [14] Abad-Manterola, Pablo (2012) Axel rover tethered dynamics and motion planning on extreme planetary terrain. Dissertation (Ph.D.), California Institute of Technology. Available on-line:
<http://resolver.caltech.edu/CaltechTHESIS:08312011-003358925>
- [15] Nagatani K, Ishida H, Yamanaka S, Tanaka Y. Three- dimensional localization and mapping for mobile robot in disaster environments. IEEE/RSJ International Conference on Intelligent Robots and Systems. Vol.4, Page(s) 3112- 3117, Las Vegas, 27-31 Oct 2003.
- [16] D. Wettergreen, C. Thorpe, and R. Whittaker. Exploring mount erebus by walking robot. Robotics and Autonomous Systems, 11(3-4):171–185, 1993.
- [17] S. Hirose and E. Fukushima, “Snakes and strings: New robotic components for rescue operations,” International Journal of Robotics Research, vol. 23, no. 4/5, pp. 341—349, 2004.
- [18] E. Mumm, S. Farritor, P. Pirjanian, C. Leger, and P. Schenker. Planetary cliff descent using cooperative robots. Autonomous Robots, 16:259–272, 2004.

- [19] Thrun, S., Fox, D., Burgard, W., & Dellaert, F. (2001). Robust Monte Carlo localization for mobile robots. *Artificial intelligence*, 128(1), 99-141.
- [20] Shang W, Sun D. Multi-sensory fusion for mobile robot self-localization. *IEEE International Conference on Mechatronics and Automation*. Page(s) 871-876, Luoyang, Henan, 25-28 June 2006.
- [21] A Nüchter, K Lingemann, J Hertzberg, Hartmut Surmann, et al. Mapping of Rescue Environments with Kurt3D, in *Proceedings of the International Workshop on Safety, Security and Rescue Robotics (SSRR '05)*, ISBN 0-7803-8946-8, Pages 158 - 163, Kobe, Japan, June 2005.
- [22] Buckham B, Nahon M. Dynamics simulation of low tension tethers, *OCEANS MTS/IEEE. Riding the Crest into the 21st Century OCEANS*. Vol.2, Page(s) 757-766, Seattle WA, USA, 1999.
- [23] Flugge W. *Handbook of Engineering Mechanics*, McGraw-Hill, New York, 1962
- [24] Vishnu Arun Kumar TR and Richardson RC. Entanglement detection of a swarm of tethered robots in search and rescue applications. *Proceedings of Fourth International Conference on Informatics in Control, Automation and Robotics (ICINCO)*. Vol. 2, Page(s) 143-148, Angers, France, 9-12 May, 2007.
- [25] Vishnu Arun Kumar TR, Richardson RC. Tether monitoring techniques for environment monitoring, tether following and localization of autonomous mobile robots. *Proceedings of IEEE/RSJ International Conference on Intelligent Robots and Systems (IROS)*. Page(s) 2109-2114, Nice, 22-26 Sept. 2008.
- [26] Van-Gessel R. The curve of a free hanging rope. <http://members.chello.nl/j.beentjes3/Ruud/catfiles/catenary.pdf>
Accessed 14 April 2011.
- [27] B.A. Abel. Underwater vehicle tether management systems. In *OCEANS'94. 'Oceans Engineering for Today's Techn. and Tomorrow's Preservation.'* Proc., volume 2, pages II/495-II/500 vol.2, 1994.
- [28] P.J. McKerrow and D. Ratner. The design of a tethered aerial robot. In *Robotics and Automation, 2007 IEEE International Conference on*, pages 355-360, 2007.